CHEMICAL ENGINEERING TRANSACTIONS
VOL. 80, 2020
A publication of AIDIC
The Italian Association of Chemical Engineering
Online at www.cetjournal.it
Guest Editors: Eliseo Maria Ranzi, Rubens Maciel Filho

ISBN 978-88-95608-78-5; **ISSN** 2283-9216
DOI: 10.3303/CET2080043

Chemical Looping Gasification of Biomass in a Bed of Geopolymeric Oxygen Carrier

Francesco Miccio*, Elena Landi, Valentina Medri, Elettra Papa, Annalisa Natali Murri

Institute of Science and Technology for Ceramics – National Research Council (CNR-ISTEC), via Granarolo 64, I-48018 Faenza (RA), Italy
francesco.miccio@cnr.it

This paper deals with a theoretical and experimental investigation on chemical looping gasification of biomass. The process was conceived by combining in a fluidized bed CO_2 gasification and oxygen delivery from a suitable oxygen carrier in order to increase the carbon conversion to CO. In such a way no dilution in nitrogen occurs and exceeding carbon dioxide can be further separated, e.g. by membrane. The results of the theoretical insights based on Cu oxide as O_2 carrier show that producer gas with heating value higher than 8 MJ/m^3 can be obtained at 900°C and equivalence ratio of 0.5. First experimental results in batch fluidized bed gasifier proved the effectiveness of a purposely developed oxygen carrier and its contribution (up to two times) in increasing the CO yield during the first stage of gasification.

1. Introduction

Gasification is awarded to be an effective route for conversion of biomass feedstock into valuable by-products for further processes of energy generation or chemical synthesis (Bridgewater, 2003). Air is the most common gaseous reactant for gasification, used at equivalence ratios ranging between 0.2 and 0.4, in order to accomplish an auto-thermal process with acceptable fuel conversion (Basu, 2006). However, the presence of nitrogen in the so-called “producer gas” penalizes its heating value and has drawbacks on its efficient utilization. Alternative to air gasification are: 1) steam or CO_2 gasification, 2) dual bed gasification; 3) oxygen gasification. In particular, oxygen gasification boasts advantages in terms of high calorific content of the producer gas and compactness of the gasifier, but would require the connection with an air separation unit. In alternative, the chemical looping gasification (CLG) of biomass can be an effective method for producing a high calorific value producer gas, with very low content of inert species (e.g. nitrogen), avoiding use of pure oxygen (Gopaul et al., 2014). So far, for a sorption enhanced CLG process, including CO_2 separation, high yield in hydrogen, up to 44 mol per kilogram of feedstock, has been predicted (Detchusananard et al., 2017).
Similar to chemical looping combustion, the CLG process needs a material able to deliver oxygen to the gasification zone, where the solid fuel is converted into a gas stream. This material, the oxygen carrier (OC), must be effective in oxygen delivery, regenerable, mechanically resistant, non-toxic and, possibly, cheap (Adanez et al., 2004). The requirements on OC toxicity is particular strong for nickel, which is even more substituted by safer metals (e.g. Fe, Mn, Cu) in industrial processes. Furthermore, the presence of the oxygen carrier, also having catalytic activity, would strongly enhance the tar conversion to lighter components (Rapagna et al., 2018).
Apart from natural metal oxides (e.g. hematite), a large number of synthetic or modified oxygen carriers based on Fe, Mn and Cu is reported in literature: instances are Fe_2O_3 on alumina support (Cabello et al., 2014); CuO promoted by Mn_2O_3 (Hosseini et al., 2015); bimetallic Mn-Fe oxides by hydrothermal synthesis (Lambert et al., 2009); promoted Fe and Mn ore by dry impregnation (Haider et al., 2016); Mn-Fe oxides embedded in geopolymer matrix (Miccio et al., 2018). The latter is a synthetic oxygen carrier easily produced by means of a one-step procedure at low temperature (below 100 °C) thanks to the advantages of the chemical consolidation of an alkali-aluminosilicate binder, namely the geopolymer matrix (Medri et al., 2013).

Paper Received: 30 November 2019; Revised: 17 February 2020; Accepted: 25 April 2020
Please cite this article as: Miccio F., Landi E., Medri V., Papa E., Natali Murri A., 2020, Chemical Looping Gasification of Biomass in a Bed of Geopolymeric Oxygen Carrier, Chemical Engineering Transactions, 80, 253-258 DOI:10.3303/CET2080043

This paper reports the results of theoretical calculations and first experiments of biomass CLG, using geopolymer based oxygen carriers. The effectiveness of the oxygen carriers (Fe/Mn and Cu/Mn) was tested in gasification conditions in a single fluidized bed reactor, operated at 900 °C under alternating regimes of gasification and regeneration. The outcomes of CLG experiments, as well as the microstructural characterization of the samples obtained from the tests are presented and discussed.

2. Materials and methods

2.1 Materials

The biomass used during the experiments was olive husk obtained from olive oil extraction in Campania (Italy). The as-received biomass was dried in hoven at 80 °C and sieved in the range 1.0-4.0 mm. The fuel properties are summarized in Table1, reporting the proximate and ultimate analyses, the low heating value (LHV) and the stoichiometric air (λ) for combustion. Before use, the biomass was devolatilized in muffle furnace at 700 °C for 1 h.

Table 1: Physical and chemical properties of olive husk

Proximate analysis		Ultimate analysis	
Moisture, %	12.4	C	54.4
Char, %	19.9	H	6.8
Volatiles, %	66.8	N	0.8
Ash, %	0.9	S	<0.1
LHV, MJ kg^{-1}	22.5	O	35.2
λ, kg/kg_{dry}	7.1		

The oxygen carrier used during the experiments was derived from previous research on chemical looping combustion of coal (Miccio et al., 2018). It is composed of a geopolymeric phase (GP) including fine powder of metal oxides (Fe_2O_3 and Mn_2O_3). In addition, a new composite geopolymer was similarly produced including copper oxide (CuO) and Mn_2O_3. The formulation and main properties of the oxygen carriers are reported in Table 2. The oxygen carriers have similar content of active phases, roughly 40%wt. The produced samples were milled in porcelain mortar and sieved in the size range 0.2-0.4 mm.

Table 2: Formulation and properties of the oxygen carriers

OC	GP, %wt	Fe_2O_3, %wt	Mn_2O_3, %wt	CuO, %wt	True density, kg m^3	Particle size, mm
GP-MnFe	59.2	27.3	13.5	0.0	1.8	0.2-0.4
GP-CuMn	63.6	0.0	24.5	11.9	2.5	0.2-0.5

2.2 Experimental technique

A bubbling fluidized bed gasifier was used for the experiments of chemical looping gasification. The tubular fluidization column was made of stainless steel (AISI-304 tube), having an internal diameter of 27 mm and total height of 600 mm. The air distributor is formed by a pack of AISI-316 wire meshes that are locked at the bottom of the tube. The top side of the column is open, allowing the biomass feeding and the connection of a suction probe for continuous gas analysis. The column was installed in a tubular furnace (Carbolite 1200) with electronic control of the temperature. The streams of gases (CO_2 , N_2 and air) were regulated by means of an electronic mass flow device (Brooks 5850S 1000L/h) and a rotameter (Key Instr. 0.5-5.0 LPM). The gas species in the exit stream, i.e. O_2, CO_2, and CO were monitored by a continuous gas analyzer (GEIT mod. 3100).

The process scheme is displayed in Figure 1. A single test was carried out with alternating steps of oxygen carrier regeneration in air flow and chemical looping gasification in CO_2 or N_2 flow. The duration of each step was between 5 and 15 min, depending on the evolution of the gas concentration profiles, as consequence of the oxygen depletion/enrichment in OC. Batches of devolatilized biomass between 0.5 and 2 g were fed during CLG step. The post-elaboration of the acquired data allowed to determine the gasification yield (η) and the heating value of the producer gas (H_v), according to equations 1 and 2, respectively, where m denotes mass flow rates and Y molar fractions in the producer gas.

$$\eta = \frac{m_{g-}m_{CO2}}{m_f} \quad (1)$$

$$H_v = Y_{CO}H_{CO} + Y_{H2}H_{H2} + Y_{CH4}H_{CH4} \quad (2)$$

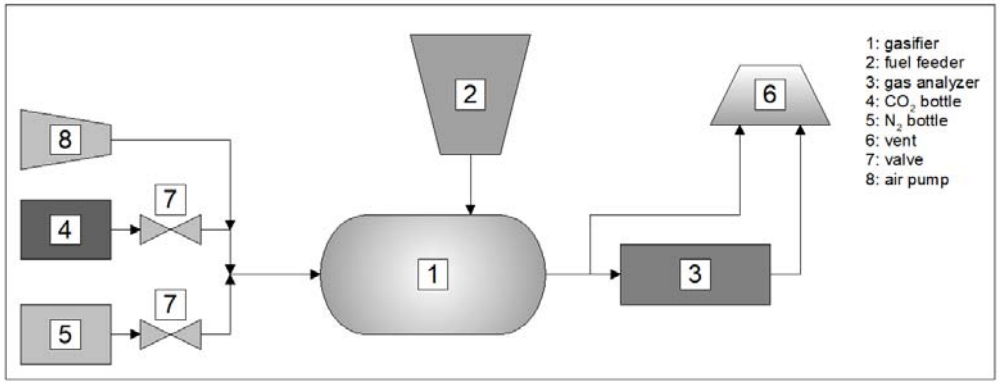

Figure 1: Process scheme of the chemical looping gasification experiment

3. Theoretical assessment

For the case of CLG with Cu oxygen carrier, CEAexec software tool by NASA (Gordon and McBride, 1994) has been used for evaluating the thermodynamic equilibrium composition of a system that is somewhat representative of the experimental tests. Since Cu oxide is more active than both Fe and Mn oxides in oxygen delivery, the estimated results should be considered as the best case for the studied CLG process.
It is worth noting that olive husk, according to its ultimate analysis (Tab. 1) and neglecting ash, can be approximated to a mixture of C (4 moles) and H_2O, (3 moles). Therefore the chemical species given as input to calculation are solely: C, H_2O, CO_2, CuO. The mole number of CuO was selected as the value corresponding to an equivalence ratio e=0.5, whilst the ratio (ψ) CO_2/C was varied from 0 to 2. It is worth noting that ψ=0 corresponds to absence of fluidization, so it does not have practical sense and should be considered as limiting condition.
CEAexec determines the equilibrium composition of the system on the basis of free-Gibbs-energy minimization, independent of the possible reactions involved in the chemical transformation. The chemical species at equilibrium are looked for in the internal database of the tool without any further input. In such case they are Cu, CO, H_2, CH_4, apart from input species C, CO_2, H_2O and CuO.

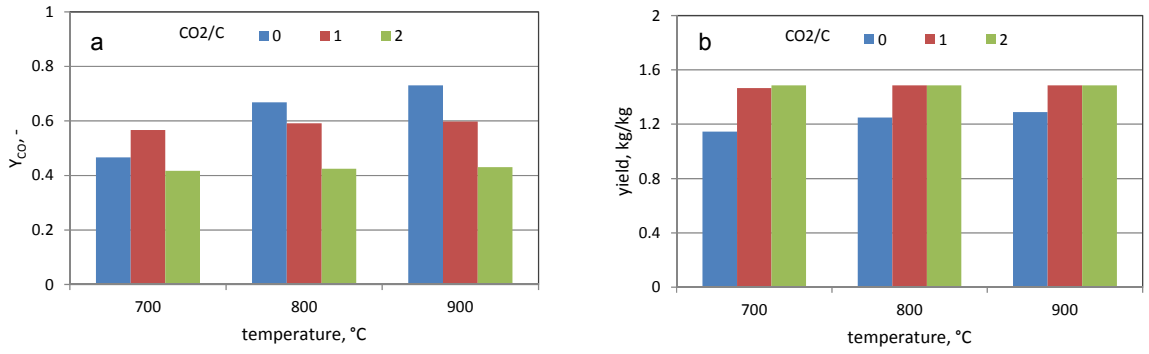

Figure 2: Results of chemical equilibrium calculations as function of T parametric in CO_2/C ratio: a) molar fraction of CO; b) producer gas yield

The results of the thermodynamic equilibrium computations are shown in Figures 2 and 3. Figure 2a displays the change with temperature of the molar fraction of CO, assumed as the most representative product of CLG, parametric in CO_2/C ratio. There is a clear increase of Y_{CO} at increasing temperature as consequence of the shift in the Boudouard reaction, favoring the conversion of solid carbon at higher temperature. The

temperature effect is attenuated by ψ increase, because of higher dilution in CO_2. Conversely, the producer gas yield increases with ψ as shown in Figure 2b.
As far as the heating value of the producer gas is concerned, Fig. 3 highlights a marked effect of T only for the case ψ =0, whilst H_v is roughly independent of temperature in the other two cases. Again, the dilution in CO_2 of the gasification products plays a major role. The heating value achieves the highest level (11.9 MJ/m^3) at T=900 °C and ψ =0, whilst it decays at increasing CO_2/C ratio. Anyway, ψ =1 yields H_v=8.3 MJ/m^3, at T=800 and 900 °C, that is acceptable for using the producer gas in a further step, e.g. internal combustion engine (Bridgewater and Evans, 1993). Therefore, the operating conditions above identified, i.e. T= 900°C, ψ =1 and e=0.5 appear to be suitable for accomplishing chemical looping gasification.
Since the equilibrium calculations were executed at assigned temperatures (i.e. 700, 800 and 900 °C), no information can be inferred about the energy balance in the examined cases.

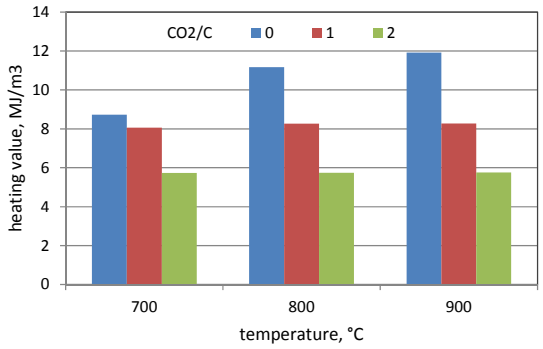

Figure 3: Results of chemical equilibrium calculations as function of T parametric in CO_2/C ratio: heating value of the producer gas

4. Results of chemical looping gasification tests

4.1 Gasification

The transient concentration profiles of CO_2, O_2 and CO downstream the CLG reactor are shown in Figures 4 and 5. In the case of GPMnFe bed (Fig. 4) a small oxygen release can be appreciated immediately after the switch from air to N_2, as revealed by the decreasing trend of the O_2 concentration after time 1500 s. The oxygen level achieved again 21% vol. in the forthcoming regeneration step in air (t=2000÷2600 s).

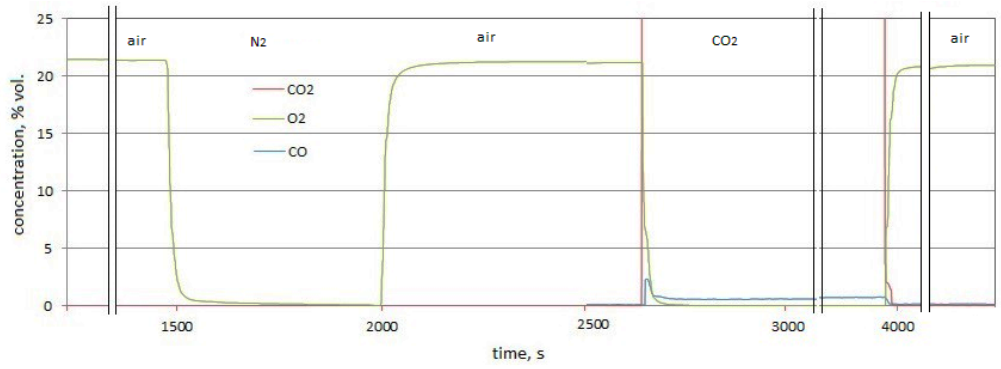

Figure 4: Concentration profiles of CO_2, O_2 and CO during a CLG test carried out with GPMnFe (T=900 °C)

At time 2700 s the switch from air to CO_2 and the contemporary feeding of fuel (0.5 g char) occurred, giving rise to a small peak of CO. However O_2 is still detected in this step, indicating that its release occurred very quickly with loss of efficiency in converting the fuel. Conversely, CO_2 attains very high level (i.e. out of the analyser range) because of its feeding at enough high rate. After O_2 depletion (t=2700÷4000 s), the fuel gasification by CO_2 occurred, as denoted by the low CO concentration (around 1% vol.) measured during this interval. The test demonstrated that only a limited fraction of carbon was gasified by oxygen supplied by GPMnFe, owing to the limited and very fast oxygen release.

Figure 5 shows the results obtained during CLG test with GPCuMn. The O_2 carrying capacity resulted much higher than GPMnFe (t=500÷5400 s) thanks to the more favorable redox behavior of Cu. However, the CO generation resulted very low during the first cycle (I) in CO_2 (t=5400÷5700 s, 1.0 g char) because the increased oxygen availability would have favoured complete conversion of C to CO_2. During the second cycle (II) in CO_2 (t=6700÷7000 s; 2.0 g char) a higher peak of CO was measured at beginning, followed by the steady C gasification by CO_2. The last step (III) was carried out in N_2 (t=7800÷8500s ; 2.0 g char), exhibiting peaks of both CO and CO_2 as consequence of the oxygen release from GPCuMn that readily reacted with the available char. By comparison of cycle II and III it can be inferred that an augmented carbon conversion to CO, around two times, occurred as an effect of combined CO_2 and OC activity during step II.

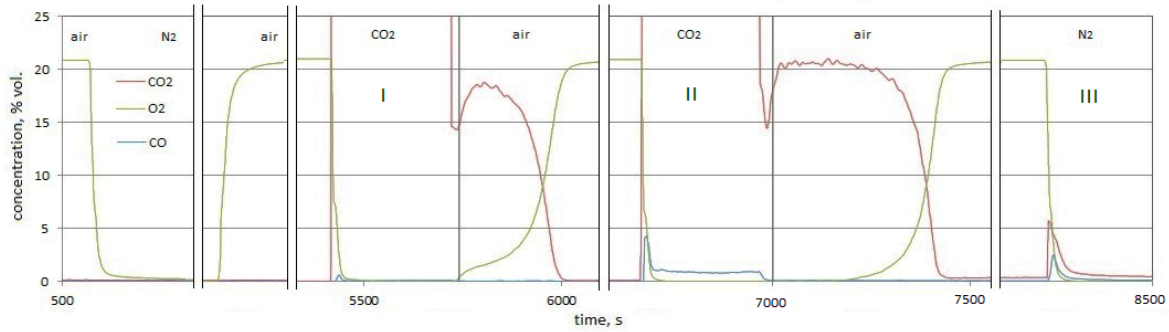

Figure 5: Concentration profiles of CO_2, O_2 and CO during a CLG test carried out with GPCuMn (T=900 °C)

4.2 Microstructural analysis

Figure 6 shows the results of the SEM characterization of the GPCuMn before and after the CLG cycle at different magnifications. No macroscopic morphological changes in the OC are evident (Fig.6A and 6C). Except for a limited shrinkage, the granules preserved an overall integrity, without showing cracking or fragmentation. At a higher magnification, the composite material displays again an intact surface (Fig.6B and 6D), thereby confirming the stability to the reaction conditions and cycling operation. The microstructure after cycling appears only more compact likely due to the operating temperature of the CLG process (900 °C) that caused a limited densification, thus confirming what evidenced at macroscopic level. However pores are still evident in the microstructure probably due to coalescence of smaller ones, as previously observed in similar materials [Miccio et al., 2018].

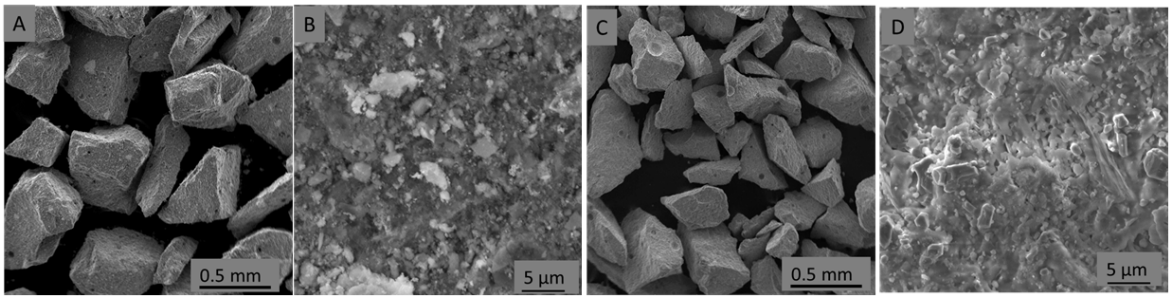

Figure 6: SEM images of GPCuMn samples before(A and B) and after (C and D) CLG test in fluidized bed at 900 °C

5. Conclusions

The chemical looping gasification of a biomass was investigated with both theoretical and experimental approaches. To this aim materials for the operation in fluidized bed have been formulated and produced adopting the green procedure of oxides inclusion inside a geopolymer matrix. The technique was successful for producing composite granules with high thermal and mechanical resistance containing up to 40%wt of oxides (Mn, Fe or Cu).

The theoretical analysis demonstrated that, at CO_2/C molar ratio equal to 1 and equivalence ratio of 0.5, the heating value can achieve values in excess of 8.0 MJ/m^3 that is acceptable for using the producer gas in a

further conversion step. However, the dilution in CO_2 (fluidizing agent) penalizes the performance of the conceived CLG process and possible separation step could be beneficial for improving the producer gas quality.
First batch experiments of CLG demonstrated the superior effectiveness of the oxygen carrier based on Cu oxide with respect to Mn/Fe oxides. The effect of OC during CO_2 gasification was proved by comparing tests in CO_2 and N_2 atmosphere, the former generating a higher peak (around double) of CO by carbon gasification and partial oxidation.
The findings of the research will provide a basic framework for the CLG investigation in a more complex configuration, i.e. steady operation of the gasifier with continuous feeding of fuel and oxygen carrier.

Acknowledgments

Dr. Mauro Mazzocchi is gratefully acknowledged for the microstructural analysis. The work was partially funded by Progetto Regionale Emilia Romagna POR-FESR 2014-2020 FireMAT (PG/2018/631345).

References

Bridgwater A.V., Renewable fuels and chemicals by thermal processing of biomass, 2003, Chem. Eng. J., 91, 87.
Basu P. (Ed.), 2006, Combustion and Gasification in Fluidized Beds, Taylor & Francis Group, LLC
Gopaul S.G., Dutta A., Clemmer R., 2014, Chemical Looping Gasification for Hydrogen Production: A Comparison of Two Unique Processes Simulated Using ASPEN Plus, Int. J. of Hydrogen Energy, 39, 5804-5817.
Detchusananard T., Ponpesh P., Saebea D., Authayanun S., Arpornwichanop A., 2017, Modeling and Analysis of Sorption Enhanced Chemical Looping Biomass Gasification, Chem. Eng. Trans., 57, 103-108.
Rapagna S., Savuto E., Di Carlo A., Gallucci K., Foscolo P.U., 2018, Integration of Biomass Gasification and Hot Gas Cleaning Processes, Chemical Engineering Transactions, 67, 661-666.
Adánez J., de Diego L.F., García-Labiano F., Gayán P., Abad A., Palacios J.M., 2004, Selection of Oxygen Carriers for Chemical-Looping Combustion, Energy & Fuels, 18, 371-377.
Cabello A., Abad A., García-Labiano F., Gayán P., de Diego L., Adánez J., 2014, Kinetic Determination of a Highly Reactive Impregnated Fe_2O_3/Al_2O_3 Oxygen Carrier for Use in Gas-Fueled Chemical Looping Combustion, Chem. Eng. J., 58, 265–280
Hosseini D., Imtiaz Q., Abdala P.M., Yoon S., Kierzkowska A.M., Weidenkaff A., Müller C.R., 2015, CuO Promoted Mn_2O_3-based Materials for Solid Fuel Combustion with Inherent CO2 Capture, Journal of Materials Chemistry A, 3, 10545-10550.
Lambert A., Delquié C., Clémeneçon I., Comte E., Lefebvre V., Rousseau J., Durand B., 2009, Synthesis and characterization of bimetallic Fe/Mn oxides for chemical looping combustion, Energy Procedia, 1, 375–381.
Haider S.K., Azimi G., Duan L., Anthony E.J., Patchigolla K., Oakey J.E., Leion H., Mattisson T., Lyngfelt A., 2016, Enhancing properties of iron and manganese ores as oxygen carriers for chemical looping processes by dry impregnation, Appl. Energy, 163, 41–50.
Miccio F., Bendoni R., Piancastelli A., Medri V., Landi E., 2018, Geopolymer Composites for Chemical Looping Combustion, Fuel, 225, 436-442.
Medri V., Landi E., Papa E., Dedecek J., Klein P., Benito P., Vaccari A., 2013, Effect of metallic Si addition on polymerization degree of in situ foamed alkali-aluminosilicates, Ceramics International, 39, 7657-7668.
Gordon S., McBride B.J., 1994, Computer Program for Calculation of Complex Chemical Equilibrium Compositions and Applications, NASA report, ref. pub. 1311.
Bridgewater A.V., Evans G.D, 1993, An Assessment of Thermochemical Conversion Systems for Processing Biomass and Refuse, ETSU B/T1/00207/REP.